### **ORGANOMETALLICS**

pubs.acs.org/Organometallics Article

# Ruthenium Phosphinimine Complex as a Fast-Initiating Olefin Metathesis Catalyst with Competing Catalytic Cycles

Sayantani Saha, Boris Averkiev, and Peter E. Sues\*

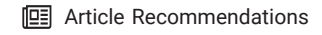


Cite This: Organometallics 2022, 41, 2879-2890



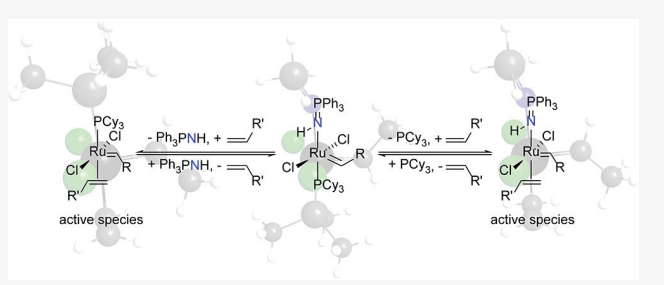
ACCESS

III Metrics & More



Supporting Information

**ABSTRACT:** A ruthenium-based olefin metathesis (OM) catalyst bearing a monodentate triphenylphosphinimine ligand, **Ru1**, was synthesized, characterized, and its activity for the homocoupling of terminal alkenes was investigated. Utilizing 1-hexene as a model substrate, the empirical rate law for **Ru1** was found to be first-order in alkene and complex (indicating that both species were involved in the rate-limiting step), with a rate constant of  $0.697 \pm 0.050$  M<sup>-1</sup> s<sup>-1</sup>. Moreover, the experimentally determined activation parameters  $\Delta S^{\ddagger}$  and  $\Delta H^{\ddagger}$  ( $-48.7 \pm 5.1$  eu and  $3.19 \pm 0.15$  kcal/mol, respectively) were consistent with an associative or associative



interchange ligand substitution reaction. When considering the  $\Delta G^{\ddagger}$  (298 K) value of 17.7 kcal/mol, Ru1 ranked among the fastest initiating ruthenium-based OM catalysts reported in the literature. Density functional theory (DFT) calculations were also performed to explore potential catalytic mechanisms. Two pathways were considered: a traditional mechanism where the phosphinimine ligand de-coordinated and an alternative mechanism where the phosphine donor de-coordinated. Although the energy differences between the two pathways were typically fairly small (1.4–3.5 kcal/mol), the alternative pathway with phosphine de-coordination was energetically more favorable. It is anticipated, however, that both cycles are working in tandem during the catalytic reaction. In addition to kinetic studies, the stability of Ru1 was explored using 1-hexene as a model substrate. The phosphinimine catalyst was found to be mildly oxygen-sensitive and moisture-tolerant. Furthermore, Ru1 was determined to be prone to bimolecular decomposition, through the crystallographic characterization of a key degradation product. There was also strong evidence for NH exchange between the tricyclohexylphosphine and triphenylphosphinimine moieties. Lastly, the substrate scope of Ru1 in regard to  $\alpha$ -olefins was explored. Catalytic efficiency dropped with more electron-deficient alkenes, as well as with increasing steric bulk on the substrate, which was consistent with the proposed catalytic mechanism.

#### ■ INTRODUCTION

The ability to build increased molecular complexity is critical for academia, as well as for many chemical industries. Therefore, methods that facilitate the selective formation of C–C bonds are highly valuable. In this context, olefin metathesis (OM) is a powerful synthetic tool. <sup>1–3</sup> One of the reasons that OM is so useful is because of its versatility; there are multiple ways to implement this transformation using the same carbene catalysts. <sup>2,4</sup> Ring-closing metathesis (RCM) is widely used in natural product syntheses, <sup>5</sup> and cross metathesis (CM) is a popular organic methodology. <sup>6</sup> Ring-opening metathesis polymerization (ROMP), on the other hand, is employed to generate polymers from cyclic, unsaturated monomers. <sup>7</sup>

Ruthenium-based Grubbs-type complexes represent one of the two main classes of catalysts that have come to dominate the field of OM.<sup>3-6</sup> There have been numerous modifications made to these systems over the years to make them more stable, as well as more selective.<sup>3-6,8-15</sup> Additionally, significant attention has been paid to generating more active Grubbs-type OM catalysts, generally through the incorporation of one or two labile ligands. These fast-initiating species

include Grubbs third-generation catalysts, <sup>16</sup> trifluoromethane-sulfonamide complexes from the Hong group, <sup>17</sup> *N*-Grubbs—Hoveyda-type systems from Plenio and co-workers, <sup>18</sup> and four-coordinate compounds from the Piers group, <sup>19,20</sup> as well as many other examples (Figure 1). <sup>21–36</sup> One commonality that all of these fast-initiating species share, and nearly all ruthenium-based OM catalysts in general, is a similar canonical structure when it comes to the active catalytic species. It is commonly accepted that the ligand *trans* to the N-heterocyclic carbene (NHC) or phosphine donor undergoes a ligand substitution reaction with the alkene substrate generating an intermediate with two anionic ligands, a phosphine or NHC ligand, a carbene donor, and a coordinated olefin (Scheme 1). <sup>3</sup> Although there are a few ruthenium-based OM precatalysts

Received: September 23, 2022 Published: October 12, 2022





**Figure 1.** Examples of fast-initiating Grubbs-type catalysts, including Grubbs third-generation catalyst (top left), a trifluoromethanesulfonamide OM catalyst (top right), an *N*-Grubbs—Hoveyda-type OM catalyst (bottom left), and a four-coordinate ruthenium-based OM catalyst (bottom right).

# Scheme 1. General Mechanism for Grubbs-Type OM Precatalyst Activation

$$\begin{array}{c|c}
L & X & -L', + \longrightarrow R' & L & X \\
X & L' & +L', - \longrightarrow R' & X & R' & NHC
\end{array}$$
pre-catalyst active species

that diverge significantly from the classic Grubbs-type structure, these complexes are still thought to form the same general active species shown in Scheme 1, in situ. <sup>37–41</sup> As such, there is still a large amount of room for innovation within the field OM, and the opportunity to unlock a new reaction manifolds through the development of ruthenium-based systems that access alternative catalytic pathways.

Phosphinimines are an underutilized class of ligands for latetransition metals that are beginning to receive more and more attention, especially as chelating donors for catalytic applications. 427 Monodentate phosphinimines, however, are quite rare on ruthenium, 43 whereas monodentate phosphinimide complexes are a bit more common. 44–53 Moreover, while phosphinimides have been utilized in early transition-metalbased alkyne metathesis,<sup>54</sup> to the best of our knowledge, phosphinimines and phosphinimides have not been used in ruthenium-based OM catalysts. What makes these ligands so intriguing is their unique electronic structure; they can act as both strong  $\sigma$ - and  $\pi$ -donors due to their ylide-like structure. Therefore, it was thought that phosphinimines and/or phosphinimides would be well suited for stabilizing high oxidation state, coordinatively unsaturated ruthenium carbene complexes that are common intermediates during OM. Additionally, phosphinimides have been used in place of cyclopentadienyl ligands for d<sup>0</sup> metallocene olefin polymerization catalysts. 56-68 A significant benefit seen for phosphinimide ligands was that they provided steric protection to the catalysts, but they also facilitated alkene binding because the bulkiness of the ligand was further removed from the metal due to the nitrogen spacer. 59 It was anticipated that phosphinimine ligands would retain many of the same steric advantages as

their anionic forms, and therefore, these species were targeted for further study.

Herein, we present the synthesis of a ruthenium phosphinimine complex and its characterization. Furthermore, the catalytic activity of the phosphinimine precatalyst for the homocoupling of terminal olefins is explored, including kinetic studies, mechanistic investigations, decomposition studies, and a brief substrate scope.

#### RESULTS AND DISCUSSION

Synthesis and Characterization of Ru1. Initial attempts to synthesize a ruthenium-based OM catalyst focused on replacing a chloride ligand in Grubbs first-generation catalyst (G1) with a phosphinimide donor. Lithium triphenylphosphinimide was generated through the deprotonation of triphenylphosphinimine (synthesized according to literature procedures)<sup>69</sup> using one equivalent of nBuLi. G1 was then treated with one equivalent of the anionic ligand, which resulted in a 50:50 mixture of G1 and a new ruthenium phosphinimine complex, according to <sup>1</sup>H NMR spectroscopy (the phosphinimide ligand became protonated, discussed further in the Supporting Information). Moreover, free tricyclohexylphosphine was evident in the <sup>31</sup>P NMR spectrum of the crude reaction mixture. To push the reaction to completion, the addition of one equivalent of silver nitrate was necessary (Scheme 2). A ruthenium phosphinimine complex, Ru1, could then be isolated as a yellow/green powder in good yield (around 49%).

Scheme 2. Synthesis of Phosphinimine Complex Ru1

The NMR spectra of **Ru1** displayed several characteristic peaks that confirmed that the proposed phosphinimine complex had been isolated. The carbene proton was evident as a doublet (coupling to the tricyclohexylphosphine ligand) around 19.7 ppm, slightly upfield shifted from **G1**. In addition, the aromatic protons for both the phenylidene and triphenylphosphinimine ligands could be detected. Most importantly, however, a broad doublet around 4.8 ppm could be seen, which corresponded to the phosphinimine N–H. With respect to the <sup>31</sup>P NMR spectrum, the expected signals could be seen: two peaks around 53 and 35 ppm for the two phosphorus-based ligands.

The structure of the precatalyst Ru1 was also confirmed by single-crystal X-ray diffraction (Figure 2). To the best of our knowledge, this compound represents the first crystallographically characterized ruthenium species with a monodentate phosphinimine donor (the N atom was trigonal planar with a Ru1A–N1A–P1A bond angle of 140.4°). With respect to bond lengths, the Ru1A–P2A distance of 2.326 Å was only slightly shortened in comparison to the ruthenium–phosphorus distances reported for G1 (2.38 and 2.35 Å), whereas the Ru1A–Cl1A, Ru1A–Cl1A, and Ru1A–C1A distances were slightly elongated. The ruthenium–phosphinimine (Ru1A–N1A) bond length of 2.08 Å, however, was shorter than the two known ruthenium structures with similar  $R_3P$ =N–H donors (2.121 and 2.109 Å). These results were quite

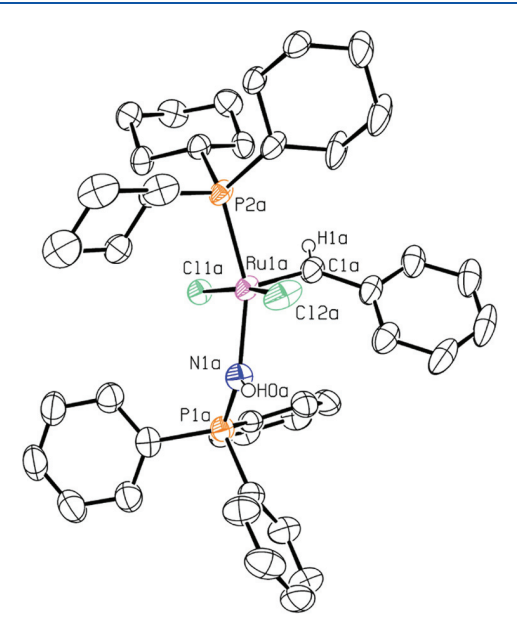


**Figure 2.** ORTEP3 representation (thermal ellipsoids at 50% probability) and atom numbering for **Ru1**, where most of the hydrogen and two other complexes that were part of the asymmetric unit were removed for clarity.

striking as it was initially anticipated that the tricyclohexylphosphine would bind much more tightly to the metal center without a *trans* phosphine donor, and that it would exert a strong *trans* influence on the triphenylphosphinimine ligand. Based on the values obtained, however, it appears that the opposite occurred: the ruthenium—phosphorus bond was not strengthened considerably, and the phosphinimine donor was tightly bound to the metal. Furthermore, these results suggest that, for these systems at least, the *trans* influence of the triphenylphosphinimine ligand was larger than expected *a priori*. Whether or not this is a general phenomenon for late-transition-metal complexes bearing these ligands requires further study. For further discussion of Ru1, as well as notable bond lengths and angles in comparison to G1, see the Supporting Information and Table S1.

Catalytic Studies Using 1-Hexene. Initial experiments evaluating the catalytic efficiency of Ru1 for OM used 1-hexene as a model substrate. Over a 2 h period, 53% 5-decene was obtained as the homocoupled product with 71% trans selectivity (Figure 3). To the best of our knowledge, no other ruthenium phosphinimine complex capable of affecting OM has previously been reported in the literature. When analyzing the reaction profiles, it immediately became apparent that there was no observable activation period at room temperature, indicating that catalyst initiation was extremely facile. This is particularly notable because many Grubbs-type OM catalysts exhibit a distinct induction period, where ligand decoordination can be rate-limiting.

To further explore these systems, kinetic investigations were conducted (also utilizing 1-hexene as a model substrate). In particular, the influence of Ru1 concentration and substrate concentration on catalytic activity was assessed using the initial rates method. The empirical rate law was found to have a first-order dependence on both substrate and catalyst, with an experimentally determined rate constant of 0.697  $\pm$  0.050  $M^{-1}$  s $^{-1}$  (Figure 4). The second-order rate law demonstrated that both the substrate and ruthenium complex were involved in

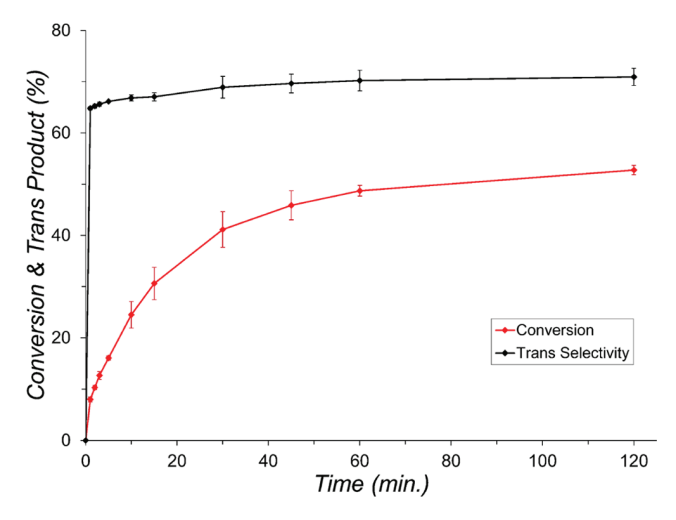
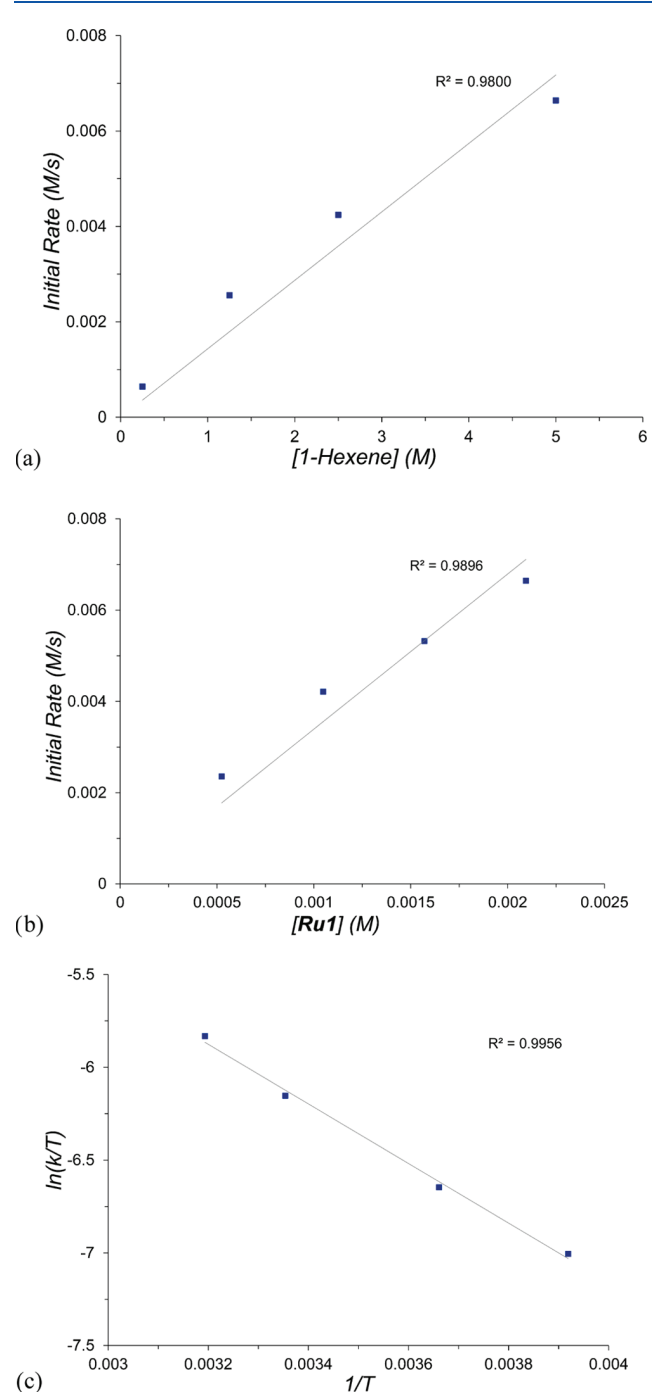


Figure 3. Reaction profile for the homocoupling of 1-hexene using Ru1 (1:2400 Ru1/1-hexene at 25  $^{\circ}$ C).

the rate-determining step. Moreover, activation parameters for the homocoupling of 1-hexene were obtained from an Eyring plot analysis, with  $\Delta S^{\ddagger}$ ,  $\Delta H^{\ddagger}$ , and  $\Delta G^{\ddagger}$  (298 K) values of  $-48.7 \pm 5.1$  eu,  $3.19 \pm 0.15$  kcal/mol, and 17.7 kcal/mol, respectively (Figure 4). In comparison to other fast-initiating ruthenium-based OM catalysts, the  $\Delta G^{\ddagger}$  (298 K) for Ru1 is around 0.4 kcal/mol smaller than the  $\Delta G^{\ddagger}$  (298 K) for the Grela nitro-substituted catalyst (18.1 kcal/mol)<sup>35,79</sup> and around 1 kcal/mol larger than the  $\Delta G^{\ddagger}$  (298 K) for the Blechert—Wakamatsu catalyst (16.7 kcal/mol). Additionally, when comparing the  $\Delta G^{\ddagger}$  (278 K) for Ru1 (16.7 kcal/mol) to the  $\Delta G^{\ddagger}$  (278 K) for Grubbs third-generation catalyst (15.45 kcal/mol), it is just over 1 kcal/mol larger. Therefore, Ru1 ranks among the fastest initiating ruthenium-based OM catalysts reported in the literature.

When examining the small enthalpy of activation for Ru1 in conjunction with the large negative entropy of activation, this suggested that there was a large decrease in disorder in the rate-limiting step with little to no bond-breaking character. In addition, the values of the experimentally determined activation parameters were consistent with those of a reported system known to undergo an associative ligand substitution reaction.<sup>82</sup> As such, this data, along with the empirical secondorder rate law, would align with an associative or an associative interchange ligand substitution reaction being the ratedetermining step. This result is significant because, as mentioned previously, the rate-limiting step for many Grubbs-type OM catalysts is ligand de-coordination.<sup>73-7</sup> Moreover, re-coordination of the original trans ligand during catalysis, thus regenerating the initial precatalyst, can decrease the concentration of active species in solution.<sup>73</sup> For systems that initiate through a dissociative mechanism, this is particularly difficult to overcome because catalyst activation is independent of olefin concentration. For Ru1, in contrast, the more substrate that is added, the more efficient the system becomes.

It is possible, however, that there are multiple competing modes of activation. Extensive research on Hoveyda—Grubbs, <sup>23–35</sup> Grubbs third-generation, <sup>81,83</sup> and a variety of other ruthenium-based OM catalysts <sup>84–86</sup> has indicated that there may be several competing initiation mechanisms (dissociative, associative, and interchange), depending on a variety of factors, including the substrate utilized (concen-



**Figure 4.** Kinetic studies investigating the homocoupling of 1-hexene using Ru1 (a) showing the rate dependence on 1-hexene concentration at 25 °C; (b) showing the rate dependence on Ru1 concentration at 25 °C; (c) showing an Eyring plot used to determine activation parameters.

tration, steric bulk, electron richness, etc.), the nature of the leaving ligand (steric bulk, electron-donating ability, etc.), as well as the overall catalyst structure. Although this may be the case for **Ru1**, based on the results and activation parameters discussed above (and the lack of saturation kinetics across a large range of substrate concentrations, up to 5 M 1-hexene)<sup>73</sup> an associative or associative interchange ligand substitution is likely the dominant mode of catalyst activation. It is hypothesized that for **Ru1**, alkene binding is facilitated by

the nitrogen spacer in the triphenylphosphinimine moiety, which places the steric bulk of the ligand further away from the metal center, much like the Stephan group saw for their phosphinimide olefin polymerization catalysts.  $^{56-68}$ 

Theoretical and Experimental Mechanistic Studies. To further explore the catalytic mechanism of Ru1, density functional theory (DFT) calculations utilizing the M11-L functional and 6-311++G\*\* (H, C, N, Cl, P) + Def2-TZVP + ECP (Ru) basis sets were performed. 87,88 A model system with hydrogen atoms in place of the phenyl groups on the phosphinimine donor and methyl groups in place of the cyclohexyl groups on the phosphine ligand, as well as in place of the substituent on the carbene moiety (to reduce computational cost) was used. Ethylene was utilized as a substrate to model catalyst initiation, metallacyclobutane formation (MCB), and cycloreversion. Two potential catalytic pathways were investigated: (1) the canonical Grubbs-type mechanism where the phosphinimine ligand trans to the phosphine de-coordinated during the catalytic cycle; (2) an alternative mechanism where the phosphine donor trans to the phosphinimine de-coordinated during the catalytic cycle (Figure 5).

For both the traditional and alternative (labels denoted by ') pathways, ethylene along with the starting complex 1 (with the phosphine and phosphinimine ligands bound to the metal center) was used as the reference point for the entire catalytic cycle. Then, associative and dissociative mechanisms for catalyst initiation were explored. It was found that dissociation of either phosphine, to give 2a, or phosphinimine, to give 2a', was associated with a large energetic penalty, with  $\Delta G_{2a}^{\circ} = 31.5$ kcal/mol and  $\Delta G_{2a'}^{\circ} = 47.0 \text{ kcal/mol}$ . In contrast, coordination of ethylene to give 2b (same structure for both pathways) was energetically favorable, with  $\Delta G_{2c}^{\circ} = -47.1$  kcal/mol. The greater than 70 or 90 kcal/mol difference between 2c and 2a or 2a', respectively, along with the kinetic results discussed above, gives strong experimental and theoretical evidence that catalyst initiation is not proceeding through a dissociative ligand substitution reaction.

For catalysis to proceed, de-coordination of one of the phosphorus-containing moieties was needed. The five-coordinate intermediates 3 and 3' were found to be significantly higher in energy than 2b, however, with  $\Delta G_3^{\circ} = -16.3$  kcal/mol and  $\Delta G_3^{\circ} = -18.7$  kcal/mol. These differences in energy ( $\Delta \Delta G^{\circ} = 30.8$  and 28.4 kcal/mol, respectively) were too large based on the experimentally determined  $\Delta G^{\ddagger}$  for the rate-determining step, and as such, we propose that the six-coordinate species 2b is not part of the catalytic cycle. Instead, it is believed that this intermediate is an off-cycle thermodynamic sink. Therefore, the DFT calculations suggest that an associative pathway for catalyst initiation would have too high of a barrier for ligand de-coordination, which points toward an associative interchange mechanism.

Upon forming 3 and 3′, OM proceeded as expected through the formation of MCB intermediates, 4 and 4′ ( $\Delta G_4^\circ = -20.9$  kcal/mol and  $\Delta G_{4'}^\circ = -29.4$  kcal/mol), followed by cycloreversion to generate a new alkene and carbene, 5 and 5′ ( $\Delta G_5^\circ = -18.0$  kcal/mol and  $\Delta G_5^\circ = -16.5$  kcal/mol). Transition states for both MCB formation, TS<sub>3,4</sub> and TS<sub>3',4'</sub>, and cycloreversion, TS<sub>3,4</sub> and TS<sub>3',4'</sub>, were found, all with relatively low energy barriers:  $\Delta G_{TS3,4}^{\ddagger} = 2.7$  kcal/mol,  $\Delta G_{TS4,5}^{\ddagger} = 11.2$  kcal/mol,  $\Delta G_{TS3',4'}^{\ddagger} = 1.6$  kcal/mol, and  $\Delta G_{TS4',5'}^{\ddagger} = 16.2$  kcal/mol. Lastly, the mechanism of alkene substitution was examined. As seen previously during catalyst initiation, olefin

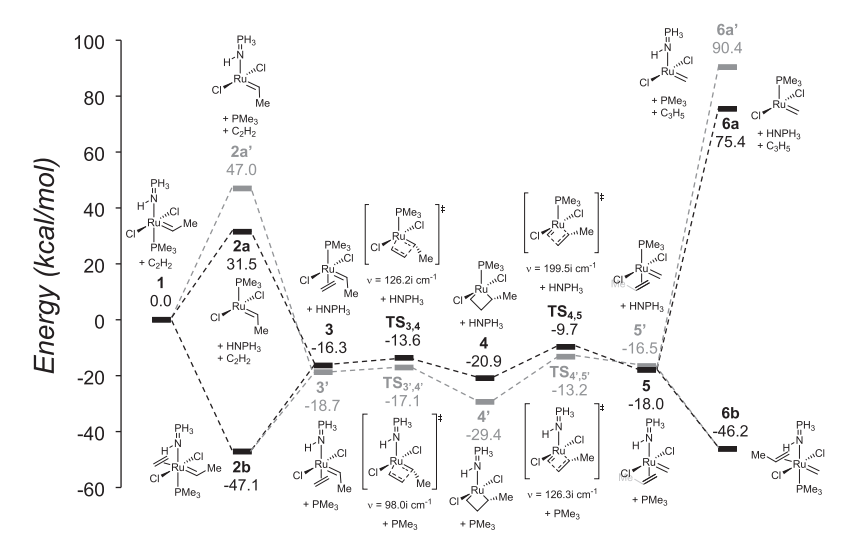


Figure 5. Free-energy profiles of the two possible OM pathways where the phosphinimine ligand de-coordinated (black) or the phosphine ligand de-coordinated (gray).

de-coordination to form four-coordinate intermediates, **6a** and **6a**', was highly disfavored with an extremely large energetic penalty,  $\Delta G_{6a}^{\circ} = 75.4 \text{ kcal/mol}$  and  $\Delta G_{6a'}^{\circ} = 90.4 \text{ kcal/mol}$ . Recoordination of the phosphinimine or the phosphine ligand, **6b** (same structure for both pathways), on the other hand, was energetically downhill ( $\Delta G_{6b}^{\circ} = -46.2 \text{ kcal/mol}$ ) and much like **2b**, is likely an off-cycle thermodynamic sink.

When analyzing the two calculated potential energy surfaces, the mechanism with de-coordination of the phosphine ligand was (for the most part) lower in energy than the more traditional pathway with de-coordination of the phosphinimine donor. Although the energy differences were not that large, typically between 1.4 and 3.5 kcal/mol, it was quite surprising that the alternative pathway was favored over the canonical Grubbs-type mechanism. The largest energy difference between the two cycles was seen between the MCB intermediates (4/4'), with a  $\Delta\Delta G^{\circ}$  value of 8.5 kcal/mol. It is possible that the strong  $\pi$ -donating ability of the phosphinimine helps stabilize alkene binding, a strong  $\pi$ -acidic ligand, in comparison to the phosphine, which is not only a strong  $\sigma$ -donor but also a  $\pi$ -acceptor (phosphines compete with alkenes for metal-ligand back-bonding). Based on these results, it is anticipated that both cycles are energetically feasible and likely working in parallel during the reaction. This is particularly exciting as it suggests that Ru1 is capable of generating an active OM species without an NHC or phosphine ligand bound. Future studies will focus on biasing the catalytic mechanism toward the alternative phosphiniminebound pathway to develop systems that can access different reaction manifolds than traditional Grubbs-type OM catalysts.

In conjunction with DFT calculations, NMR-scale reactions with 1:20 Ru1/1-hexene were carried out. After 5 min, when analyzing the carbene region of the <sup>1</sup>H NMR spectrum (Figures S8 and S9), a small amount of starting material was present in solution, along with two major species (a doublet as well as a doublet of triplets) and one minor species (a triplet). The doublet was consistent with a methylidene complex, while the doublet of triplets was consistent with a pentylidene intermediate (both with a coordinated tricyclohexylphosphine ligand). The minor triplet, on the other hand, was tentatively assigned as a pentylidene complex with no phosphine bound,

which gives some evidence for the alternative mechanism discussed above. These assignments were supported by the <sup>31</sup>P NMR spectrum, which displayed two large phosphorus peaks at 63.7 and 57.5 ppm, corresponding to two chemically distinct triphenylphosphinimine ligands bound to ruthenium, and two large signals at 36.0 and 35.4 ppm, corresponding to coordinated tricyclohexylphosphine ligands. There were a few other minor species in solution, but no free tricyclohexylphosphine or triphenylphosphinimine could be detected. Based on these results, the two major species that were spectroscopically observed are either five- or six-coordinate ruthenium complexes with both phosphorus-containing ligands bound to the metal center. This agrees with the resting states predicted by the DFT calculations (structures 2b and 6b), which were the same for either of the mechanisms that were explored. After 20 min, it was observed that the two major species decreased in intensity, whereas the minor species increased in intensity (Figures S8 and S9).

**Examining Catalyst Stability.** In addition to the kinetic and mechanistic experiments discussed above, 1-hexene was used as a model substrate to investigate the air and moisture sensitivity of the phosphinimine systems (Figure 6). For case I, the homocoupling of 1-hexene was carried out using a mixture of dried/degassed 1-hexene (2400 equiv, 10 mmol) and a solution of precatalyst Ru1 (1 equiv, 0.004 mmol) in 0.4 mL dried/degassed CDCl<sub>3</sub> (Figure 6). When the reaction was performed, however, it was opened to air. These conditions were meant to determine the oxygen sensitivity of the active catalyst, and 71% trans selectivity for 5-decene was obtained with an overall conversion of 53% after 2 h (initial turnover frequency, TOF, of 11,500  $\pm$  400 h<sup>-1</sup>). Next, for case II, the reaction was carried out in air using benchtop CDCl<sub>3</sub> and 1hexene (the same 1:2400 ratio of Ru1/1-hexene was utilized, Figure 6). A 48% conversion after 2 h was obtained, with 71% selectivity for trans-5-decene (initial TOF of 8200  $\pm$  500 h<sup>-1</sup>). Although there was a decrease in initial TOF on going from case I to case II (between 20 and 30%), over 2 h there was not a large difference between using dried and benchtop solvents/ substrates outside of a glovebox atmosphere. In contrast, for case III, the reaction was conducted inside of a glovebox using dried/degassed 1-hexene and CDCl<sub>3</sub> (Figure 6). A 69%

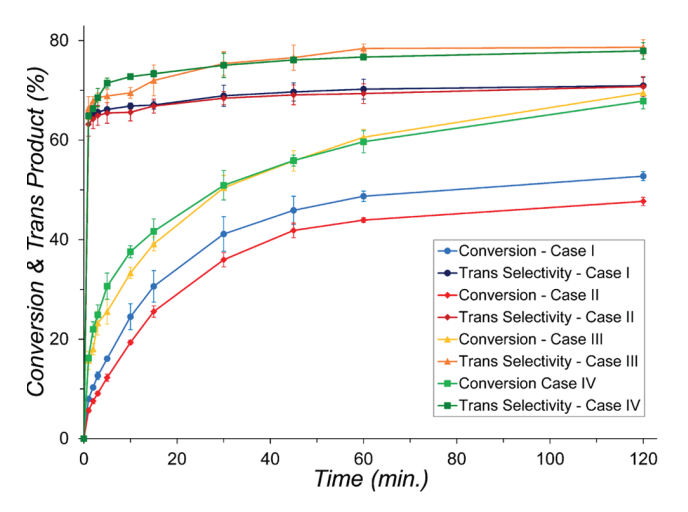
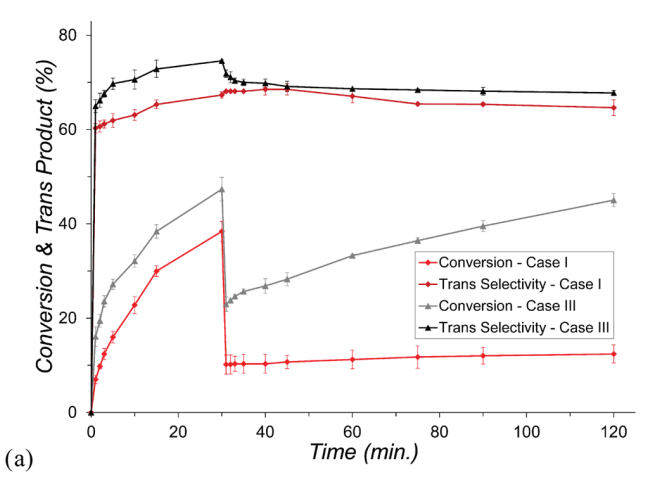


Figure 6. Reaction profiles for the homocoupling of 1-hexene using Ru1 (1:2400 Ru1/1-hexene at 25  $^{\circ}$ C) under various conditions.

conversion after 2 h was obtained, with 79% selectivity for *trans*-5-decene (initial TOF of 22,600  $\pm$  1300 h $^{-1}$ ). This represented a substantial increase in initial TOF (approximately 100% increase), as well as higher conversion and *trans* selectivity over a 2 h period (in comparison to cases I and II). Lastly, for case IV, catalysis was also carried out under a glovebox atmosphere, but degassed benchtop 1-hexene and CDCl $_3$  were utilized (not dried, Figure 6). A 68% conversion after 2 h was obtained, with 78% selectivity for *trans*-5-decene (initial TOF of 23,300  $\pm$  300 h $^{-1}$ ). As such, case III and case IV were the same within error, suggesting that **Ru1** was mildly oxygen-sensitive but not moisture-sensitive.

To further support the hypothesis that catalyst decomposition in air caused the observed decrease in activity, additional studies using conditions similar to case I and case III were carried out. In the first set of experiments, catalysis was allowed to proceed normally, except that after 30 min (typically where catalytic activity dropped and conversion began to plateau), more substrate (2400 equiv) was added (Figure 7a). It was clear that under an inert atmosphere, the active catalyst was still present in solution and continued to convert 1-hexene to 5-decene. The reactions conducted in the presence of oxygen, in contrast, showed almost no conversion after the addition of more substrate. For the second set of experiments, catalysis was once again allowed to proceed normally, under conditions similar to case I, except that after 30 min, more catalyst (1 equiv) was added (Figure 7b). This caused a rapid increase in conversion, which once again began to plateau over time (30 min after the 2nd equiv of catalyst was injected, or after 60 min total). These results gave strong evidence that catalyst decomposition in air and not substrate consumption was responsible for the observed loss of activity over time. Interestingly, the protocol with sequential addition of the catalyst displayed 68% conversion after 2 h, with 78% selectivity for trans-5-decene, much like case III and case IV in Figure 6.

Although  $\mathbf{Ru1}$  was found to be relatively stable in solution at room temperature over several days, after longer periods of time, the precatalyst was found to slowly decompose. To probe potential decomposition pathways, a solution of  $\mathbf{Ru1}$  in toluene was allowed to sit for 1 week in a glovebox and was then cooled to -30 °C. After approximately one more week had elapsed, crystals suitable for single-crystal X-ray diffrac-



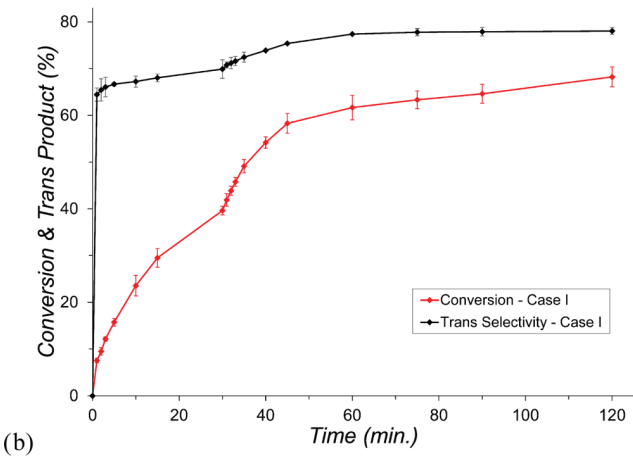


**Figure 7.** Reaction profiles for the homocoupling of 1-hexene using **Ru1** (1:2400 **Ru1**/1-hexene at 25 °C), where after 30 min, an additional (a) 2400 equiv of 1-hexene were added; (b) 1 equiv of **Ru1** was added

tometry were obtained. The structure of the decomposition product, Ru2, displayed a piano stool structure with two chlorides, a triphenylphosphine ligand, and an  $\eta^6$ -trans-stilbene moiety (Figure 8). For notable bond lengths and angles for Ru2, as well as a brief discussion, see the Supporting Information.

The structure of Ru2 was quite informative as to the potential decomposition pathways for Ru1. What immediately became apparent was that the ruthenium center had been reduced to Ru(II), and the carbene ligand, as well as the tricyclohexylphosphine moiety, was missing. In addition, the triphenylphosphinimine had been reduced to a triphenylphosphine donor. A major key in rationalizing these transformations was the presence of the stilbene ligand. This gave compelling evidence for a bimolecular mechanism of decomposition, which is well documented with Schrock-type OM catalysts<sup>1,89,90</sup> but also known for ruthenium systems.<sup>91</sup> With respect to the appearance of the triphenylphosphine ligand in conjunction with the disappearance of the tricyclohexylphosphine donor, it is anticipated that the NH functionality was exchanged onto the more electron-rich phosphorus atom, similar to the way phosphine oxides and phosphines can exchange oxygen atoms. 94 In support of this hypothesis, DFT calculations showed that the formation of tricyclohexylphosphinimine was thermodynamically favorable

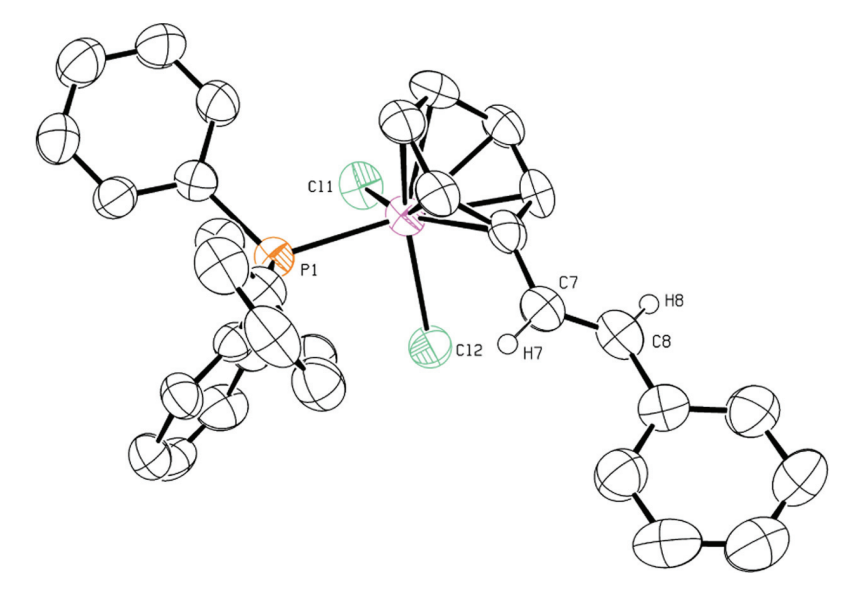


Figure 8. ORTEP3 representation (thermal ellipsoids at 50% probability) and atom numbering for Ru2, where most of the hydrogens were removed for clarity.

(2.7 kcal/mol downhill, see the Supporting Information for more details). While these calculations suggest that the proposed NH transfer would be thermodynamically feasible, the specific mechanism of action is currently unknown. There are multiple potential species in solution that could catalyze this transfer, or there could also be a mechanism with direct transfer of the NH moiety. More studies are needed.

**Substrate Scope Investigations.** After completing the mechanistic studies above, the substrate scope of **Ru1** with respect to terminal alkenes was explored (Scheme 3 and Table

Scheme 3. Homocoupling of Terminal Alkenes Catalyzed by Ru1

1). All reactions were carried out under a glovebox atmosphere at room temperature in CDCl3. The homocoupling of 1hexene was carried out using an 1:100 ratio of Ru1/substrate for comparison purposes (Table 1, entry 1). After 2 h, a 77.8% conversion was obtained with 83% trans product. After stirring the reaction mixture for an additional 22 h, 91% 5-decene was afforded with 82% trans selectivity. To examine the effects of steric bulk, progressively more encumbered substrates 4methyl-1-pentene, 3-methylpent-1-ene, and 3,3-dimethyl-1butene were examined. For the least sterically hindered substrate, 4-methyl-1-pentene, conversions of 75.3% (2 h) and 78.2% (24 h) were obtained with 74% and 79% trans selectivity, respectively (Table 1, entry 2). It was hypothesized that catalyst decomposition caused the incomplete conversion after 24 h, so an additional equivalent of Ru1 was added, and the mixture was left stirring for a further 24 h. After 48 h, 86.8% conversion was obtained with 78% trans product (overall 1:50 ratio of Ru1/substrate). Following the same procedure, 3-methylpent-1-ene provided 34.6% overall conversion after 48 h with >99% trans selectivity (Table 1, entry 3), while 3,3-dimethyl-1-butene gave <1% conversion (Table 1, entry 4). A clear trend was observed, where catalytic efficiency dropped from entries 1 to 4, correlating with an

increase in substrate steric bulk. This phenomenon can be rationalized based on the proposed catalytic mechanism: more sterically hindered substrates are less likely to engage in an associative-type ligand substitution reactions. Additionally, substrates that are too large and require a dissociative pathway for metal binding (such as 3,3-dimethyl-1-butene) are unlikely to engage in OM with Ru1.

To examine the functional group tolerance of Ru1, hex-5-en-2-one, allyl acetate, and allylamine were investigated. A similar procedure to the one used for entries 2 to 4 in Table 1 was employed. The presence of the carbonyl group reduced both the overall conversion, 48.7%, and trans selectivity, 73% (Table 1, entry 5). Allyl acetate also demonstrated comparable results (Table 1, entry 6). The presence of an amine, however, caused a dramatic reduction in catalytic activity with 7.4% conversion over a 48 h period. We are unsure at this time why Ru1 exhibited diminished catalytic ability with these substrates, but in regard to allylamine, sensitivity to protic functional groups can likely be ruled out as wet solvents could be utilized for the homocoupling of 1-hexene without a decrease in activity. It is possible that coordination of the Lewis basic groups could be responsible for the reduced catalytic efficiency, but further studies are needed.

Lastly, styrene and several of its para-substituted derivatives were tested using the protocol established for entries 2 to 7. The more electron-rich substrates, including styrene, paramethylstyrene, and para-methoxystyrene (Table 1, entries 8 to 10), showed higher conversions (between 27.8 and 29.5% after 24 h) with almost perfect trans selectivity (>99%). The styrene derivatives with electron-withdrawing groups, on the other hand, para-fluorostyrene and para-nitrostyrene (Table 1, entries 11 and 12), became progressively less reactive, the more electron-poor the alkene, with conversions of 22.9 and 9.3% after 24 h, respectively (>99% trans selectivity still maintained). The overall trend seen with the styrene substrates showed good agreement with the proposed catalytic mechanism, where an associative interchange ligand substitution reaction was hypothesized to be the rate-limiting step. More electron-poor substrates would be less effective for this catalytic pathway (styrenes in general are more electron-

Table 1. Substrate Scope of Ru1 for the Homocoupling of Terminal Alkenes<sup>a</sup>

| Entry Substrate |                  | Conversion (%) |              |            | Selectivity (% trans) |      |      |
|-----------------|------------------|----------------|--------------|------------|-----------------------|------|------|
| Entry           | Substrate        | 2 h            | 24 h         | 48 h       | 2 h                   | 24 h | 48 h |
| $1^b$           | ~~//             | 77.8           | 90.9         | -          | 83                    | 82   | _    |
| 2               |                  | 75.3           | 78.2         | 86.8       | 74                    | 79   | 78   |
| 3               |                  | 12.3           | 21.9         | 34.6       | >99                   | >99  | >99  |
| 4               |                  | <1             | <1           | <1         | _                     | -    | _    |
| 5               |                  | 36.7           | 40.1         | 48.7       | 71                    | 70   | 73   |
| 6               |                  | 39.8           | 42.9         | 52.2       | 83                    | 81   | 79   |
| 7               | $H_2N$           | <3             | 6.5          | 7.4        | _                     | 71   | 75   |
| <b>8</b> c      |                  | 10.5           | 29.5         | 28.4       | >99                   | >99  | >99  |
| Ü               |                  |                | $(22.1)^d$   | $(61.1)^d$ |                       |      |      |
| <b>9</b> c      |                  | 10.3           | 27.8         | 20.6       | >99                   | >99  | >99  |
|                 |                  |                | $(31.9)^{d}$ | $(69.1)^d$ |                       |      |      |
| 10 <sup>c</sup> | \ <u>\</u>       | 10.2           | 28.7         | 21.3       | >99                   | >99  | >99  |
|                 |                  |                | $(18.5)^d$   | $(55.6)^d$ |                       |      |      |
| 11 <sup>c</sup> | F—               | 6.5            | 22.9         | 18.7       | >99                   | >99  | >99  |
| ••              |                  |                | $(37.4)^d$   | $(76.6)^d$ |                       |      |      |
| 12 <sup>c</sup> | O <sub>2</sub> N | 3.1            | 9.3          | 8.2        | >99                   | >99  | >99  |
|                 |                  |                | $(17.5)^d$   | $(55.7)^d$ |                       |      |      |

<sup>a</sup>Reaction conditions: 0.61 M substrate, 12.2 mM precatalyst Ru1 (two additions of Ru1) in CDCl<sub>3</sub> at room temperature; yields, as well as *cis/trans* selectivity were determined by <sup>1</sup>H NMR spectroscopy of the crude reaction mixtures. <sup>b</sup>Ru1 (6.1 mM) was used. <sup>c</sup>1,3,5-Trimethoxybenzene (0.61 M) was used as an internal standard. <sup>d</sup>Percentage of substrate/product consumed to generate polymerization side products.

deficient than 1-hexene), which was clearly shown by parafluorostyrene and para-nitrostyrene. In addition, it should be noted that in all cases (Table 1, entries 8 to 12), polymerization products formed in addition to the desired homocoupled species, which was verified using an internal standard (1,3,5-trimethoxybenzene). This likely contributed to the modest conversions seen for all of the styrene substrates. It is believed that the decomposition products of Ru1 are responsible for this observation as it has been reported that para-cymene ruthenium complexes, which are similar in structure to Ru2, are capable of affecting styrene polymerization. 95

#### CONCLUSIONS

In summary, a ruthenium phosphinimine OM catalyst, **Ru1**, was synthesized, fully characterized, and its activity for the homocoupling of terminal alkenes was explored. Using 1-hexene as a model substrate, the experimentally determined rate law was found to be first-order in substrate and catalyst, indicating that both species were involved in the rate-determining step. Moreover, the empirical activation parameters  $\Delta S^{\ddagger}$  and  $\Delta H^{\ddagger}$  were consistent with an associative-type

ligand substitution reaction. <sup>82</sup> When considering the  $\Delta G^{\ddagger}$  (298 K) value of Ru1, it ranked among the fastest initiating ruthenium-based OM catalysts, including the Grela nitrosubstituted catalyst, <sup>35,79</sup> the Blechert–Wakamatsu catalyst, <sup>31,80</sup> and Grubbs third-generation catalyst. <sup>81</sup> DFT calculations were also performed to further explore the catalytic mechanism. Two potential energy surfaces were investigated: one where the phosphinimine ligand de-coordinated (traditional mechanism) and the other where the phosphine donor decoordinated (alternative mechanism). Although the energy differences between the two pathways were not that large, the canonical Grubbs-type mechanism was less energetically favorable than the alternative pathway. Furthermore, the theoretical calculations matched well with experimental data and were further supported by NMR-scale reactions.

In addition to kinetic and mechanistic experiments, the stability of Ru1 was explored. Once again using 1-hexene as a model substrate, the phosphinimine OM catalyst was found to be somewhat oxygen-sensitive but not overly moisture-sensitive. A key decomposition product of Ru1 was also crystallographically characterized, Ru2, which gave insight into the phosphinimine catalyst's decomposition pathways. Ru2

gave strong evidence for a bimolecular mechanism of decomposition, as well as NH exchange between the tricyclohexylphosphine and triphenylphosphinimine moieties (supported by DFT calculations). Lastly, the substrate scope of Ru1 with respect to terminal olefins was explored. Two clear trends were observed: catalytic efficiency dropped with increasing steric bulk on the substrate, as well as with more electron-poor alkenes. These results were consistent with the proposed catalytic mechanism, where an associative interchange ligand substitution reaction would be hindered by sterically encumbered and/or electron-deficient olefins. Future studies with phosphinimine OM systems will focus on favoring the alternative phosphinimine-bound catalytic pathway to access different reaction manifolds than traditional Grubbstype OM catalysts.

#### ASSOCIATED CONTENT

#### **Supporting Information**

The Supporting Information is available free of charge at https://pubs.acs.org/doi/10.1021/acs.organomet.2c00487.

Experimental and NMR spectra, discussion of Ru1 formation, discussion of Ru1 and Ru2 crystal structures, reaction profiles and kinetic analyses, NMR-scale reaction with Ru1 and 1-hexene, ground state energies of triphenylphosphinimine versus tricyclohexylphosphinimine, representative <sup>1</sup>H NMR spectra for terminal olefin homocoupling (PDF)

Cartesian coordinates and free energies of optimized structures (XYZ)

#### **Accession Codes**

CCDC 2205902—2205903 contain the supplementary crystallographic data for this paper. These data can be obtained free of charge via www.ccdc.cam.ac.uk/data\_request/cif, or by emailing data\_request@ccdc.cam.ac.uk, or by contacting The Cambridge Crystallographic Data Centre, 12 Union Road, Cambridge CB2 1EZ, UK; fax: +44 1223 336033.

#### AUTHOR INFORMATION

#### **Corresponding Author**

Peter E. Sues — Department of Chemistry, Kansas State University, Manhattan, Kansas 66503, United States; orcid.org/0000-0002-3975-119X; Email: psues@ksu.edu

#### **Authors**

Sayantani Saha — Department of Chemistry, Kansas State University, Manhattan, Kansas 66503, United States Boris Averkiev — Department of Chemistry, Kansas State University, Manhattan, Kansas 66503, United States

Complete contact information is available at: https://pubs.acs.org/10.1021/acs.organomet.2c00487

#### **Notes**

The authors declare no competing financial interest.

#### ACKNOWLEDGMENTS

This work was supported by the National Science Foundation (Grant Numbers CHE-2018414 and CHE-1826982), which provided funding used to purchase the single-crystal X-ray diffractometer and associated software employed in this study, as well as the Bruker 400 MHz spectrometer. The authors would also like to thank Dr. William Brennessel from the

CENTC Elemental Analysis Facility at the University of Rochester for performing the elemental analyses.

#### REFERENCES

- (1) Schrock, R. R. Multiple Metal—Carbon Bonds for Catalytic Metathesis Reactions (Nobel Lecture). *Angew. Chem., Int. Ed.* **2006**, 45, 3748—3759.
- (2) Chauvin, Y. Olefin Metathesis: The Early Days (Nobel Lecture). *Angew. Chem., Int. Ed.* **2006**, *45*, 3740–3747.
- (3) Grubbs, R. H. Olefin-Metathesis Catalysts for the Preparation of Molecules and Materials (Nobel Lecture). *Angew. Chem., Int. Ed.* **2006**, *45*, 3760–3765.
- (4) Vougioukalakis, G. C.; Grubbs, R. H. Ruthenium-Based Heterocyclic Carbene-Coordinated Olefin Metathesis Catalysts. *Chem. Rev.* **2010**, *110*, 1746–1787.
- (5) Lee, C. W.; Grubbs, R. H. Stereoselectivity of Macrocyclic Ring-Closing Olefin Metathesis. *Org. Lett.* **2000**, *2*, 2145–2147.
- (6) Chatterjee, A. K.; Choi, T.-L.; Sanders, D. P.; Grubbs, R. H. A General Model for Selectivity in Olefin Cross Metathesis. *J. Am. Chem. Soc.* **2003**, *125*, 11360–11370.
- (7) Schrock, R. R. Synthesis of stereoregular ROMP polymers using molybdenum and tungsten imido alkylidene initiators. *Dalton Trans.* **2011**, *40*, 7484–7495.
- (8) Hoveyda, A. H. Evolution of Catalytic Stereoselective Olefin Metathesis: From Ancillary Transformation to Purveyor of Stereochemical Identity. *J. Org. Chem.* **2014**, *79*, 4763–4792.
- (9) Xu, C.; Liu, Z.; Torker, S.; Shen, X.; Xu, D.; Hoveyda, A. H. Synthesis of Z- or E-Trisubstituted Allylic Alcohols and Ethers by Kinetically Controlled Cross-Metathesis with a Ru Catechothiolate Complex. J. Am. Chem. Soc. 2017, 139, 15640–15643.
- (10) Luo, S.-X.; Cannon, J. S.; Taylor, B. L. H.; Engle, K. M.; Houk, K. N.; Grubbs, R. H. Z-Selective Cross-Metathesis and Homodimerization of 3E-1,3-Dienes: Reaction Optimization, Computational Analysis, and Synthetic Applications. *J. Am. Chem. Soc.* **2016**, *138*, 14039—14046.
- (11) Xu, C.; Shen, X.; Hoveyda, A. H. In Situ Methylene Capping: A General Strategy for Efficient Stereoretentive Catalytic Olefin Metathesis. The Concept, Methodological Implications, and Applications to Synthesis of Biologically Active Compounds. *J. Am. Chem. Soc.* 2017, 139, 10919–10928.
- (12) Jung, K.; Kang, E.-H.; Sohn, J.-H.; Choi, T.-L. Highly  $\beta$ -Selective Cyclopolymerization of 1,6-Heptadiynes and Ring-Closing Enyne Metathesis Reaction Using Grubbs Z-Selective Catalyst: Unprecedented Regioselectivity for Ru-Based Catalysts. *J. Am. Chem. Soc.* **2016**, *138*, 11227–11233.
- (13) Smit, W.; Ekeli, J. B.; Occhipinti, G.; Woźniak, B.; Törnroos, K. W.; Jensen, V. R. Z-Selective Monothiolate Ruthenium Indenylidene Olefin Metathesis Catalysts. *Organometallics* **2020**, *39*, 397–407.
- (14) Montgomery, T. P.; Johns, A. M.; Grubbs, R. H. Recent Advancements in Stereoselective Olefin Metathesis Using Ruthenium Catalysts. *Catalysts* **2017**, *7*, 87.
- (15) Müller, D. S.; Baslé, O.; Mauduit, M. A tutorial review of stereoretentive olefin metathesis based on ruthenium dithiolate catalysts. *Beilstein J. Org. Chem.* **2018**, *14*, 2999–3010.
- (16) Love, J. A.; Morgan, J. P.; Trnka, T. M.; Grubbs, R. H. A Practical and Highly Active Ruthenium-Based Catalyst that Effects the Cross Metathesis of Acrylonitrile. *Angew. Chem., Int. Ed.* **2002**, *41*, 4035–4037.
- (17) Song, K.; Kim, K.; Hong, D.; Kim, J.; Heo, C. E.; Kim, H. I.; Hong, S. H. Highly active ruthenium metathesis catalysts enabling ring-opening metathesis polymerization of cyclopentadiene at low temperatures. *Nat. Commun.* **2019**, *10*, No. 3860.
- (18) Peeck, L. H.; Savka, R. D.; Plenio, H. Fast Olefin Metathesis at Low Catalyst Loading. *Chem. Eur. J.* 2012, 18, 12845–12853.
- (19) Romero, P. E.; Piers, W. E.; McDonald, R. Rapidly Initiating Ruthenium Olefin-Metathesis Catalysts. *Angew. Chem., Int. Ed.* **2004**, 43, 6161–6165.
- (20) Leitao, E. M.; Dubberley, S. R.; Piers, W. E.; Wu, Q.; McDonald, R. Thermal Decomposition Modes for Four-Coordinate

- Ruthenium Phosphonium Alkylidene Olefin Metathesis Catalysts. Chem. Eur. J. 2008, 14, 11565–11572.
- (21) Occhipinti, G.; Törnroos, K. W.; Jensen, V. R. Pyridine-Stabilized Fast-Initiating Ruthenium Monothiolate Catalysts for Z-Selective Olefin Metathesis. *Organometallics* **2017**, *36*, 3284–3292.
- (22) Ahmed, T. S.; Grubbs, R. H. Fast-Initiating, Ruthenium-based Catalysts for Improved Activity in Highly E-Selective Cross Metathesis. *J. Am. Chem. Soc.* **2017**, *139*, 1532–1537.
- (23) Vorfalt, T.; Wannowius, K.-J.; Plenio, H. Probing the Mechanism of Olefin Metathesis in Grubbs—Hoveyda and Grela Type Complexes. *Angew. Chem., Int. Ed.* **2010**, *49*, 5533—5536.
- (24) Dang, Y.; Wang, Z.-X.; Wang, X. A Thorough DFT Study of the Mechanism of Homodimerization of Terminal Olefins through Metathesis with a Chelated Ruthenium Catalyst: From Initiation to Z Selectivity to Regeneration. *Organometallics* **2012**, *31*, 7222–7234.
- (25) Nuñez-Zarur, F.; Solans-Monfort, X.; Rodríguez-Santiago, L.; Sodupe, M. Differences in the Activation Processes of Phosphine-Containing and Grubbs—Hoveyda-Type Alkene Metathesis Catalysts. *Organometallics* **2012**, *31*, 4203–4215.
- (26) Thiel, V.; Hendann, M.; Wannowius, K.-J.; Plenio, H. On the Mechanism of the Initiation Reaction in Grubbs-Hoveyda Complexes. J. Am. Chem. Soc. 2012, 134, 1104-1114.
- (27) Ashworth, I. W.; Hillier, I. H.; Nelson, D. J.; Percy, J. M.; Vincent, M. A. Olefin Metathesis by Grubbs—Hoveyda Complexes: Computational and Experimental Studies of the Mechanism and Substrate-Dependent Kinetics. *ACS Catal.* **2013**, *3*, 1929–1939.
- (28) Nelson, D. J.; Queval, P.; Rouen, M.; Magrez, M.; Toupet, L.; Caijo, F.; Caijo, F.; Borré, E.; Borré, E.; Laurent, I.; Laurent, I.; Crévisy, C.; Crévisy, C.; Baslé, O.; Baslé, O.; Mauduit, M.; Mauduit, M.; Percy, J. M. Synergic Effects Between N-Heterocyclic Carbene and Chelating Benzylidene—Ether Ligands Toward the Initiation Step of Hoveyda—Grubbs Type Ru Complexes. ACS Catal. 2013, 3, 259—264.
- (29) Bieszczad, B.; Barbasiewicz, M. The Key Role of the Nonchelating Conformation of the Benzylidene Ligand on the Formation and Initiation of Hoveyda—Grubbs Metathesis Catalysts. *Chem. Eur. J.* **2015**, 21, 10322–10325.
- (30) Griffiths, J. R.; Keister, J. B.; Diver, S. T. From Resting State to the Steady State: Mechanistic Studies of Ene—Yne Metathesis Promoted by the Hoveyda Complex. *J. Am. Chem. Soc.* **2016**, *138*, 5380–5391.
- (31) Trzaskowski, B.; Goddard, W. A.; Grela, K. Faster initiating olefin metathesis catalysts from introducing double bonds into cyclopropyl, cyclobutyl and cyclopentyl derivatives of Hoveyda-Grubbs precatalysts. *Mol. Catal.* **2017**, *433*, 313–320.
- (32) Zieliński, A.; Szczepaniak, G.; Gajda, R.; Woźniak, K.; Trzaskowski, B.; Vidović, D.; Kajetanowicz, A.; Grela, K. Ruthenium Olefin Metathesis Catalysts Systematically Modified in Chelating Benzylidene Ether Fragment: Experiment and Computations. *Eur. J. Inorg. Chem.* **2018**, 2018, 3675–3685.
- (33) Albalawi, M. O.; Falivene, L.; Jedidi, A.; Osman, O. I.; Elroby, S. A.; Cavallo, L. Influence of the anionic ligands on properties and reactivity of Hoveyda-Grubbs catalysts. *Mol. Catal.* **2021**, *509*, No. 111612.
- (34) Luo, S.-X.; Engle, K. M.; Dong, X.; Hejl, A.; Takase, M. K.; Henling, L. M.; Liu, P.; Houk, K. N.; Grubbs, R. H. An Initiation Kinetics Prediction Model Enables Rational Design of Ruthenium Olefin Metathesis Catalysts Bearing Modified Chelating Benzylidenes. *ACS Catal.* **2018**, *8*, 4600–4611.
- (35) Trzaskowski, B.; Ostrowska, K. A computational study of structures and catalytic activities of Hoveyda-Grubbs analogues bearing coumarin or isopropoxycoumarin moiety. *Catal. Commun.* **2017**, *91*, 43–47.
- (36) Kajetanowicz, A.; Grela, K. Nitro and Other Electron Withdrawing Group Activated Ruthenium Catalysts for Olefin Metathesis Reactions. *Angew. Chem., Int. Ed.* **2021**, *60*, 13738–13756. (37) Fürstner, A.; Liebl, M.; Lehmann, C. W.; Picquet, M.; Kunz, R.; Bruneau, C.; Touchard, D.; Dixneuf, P. H. Cationic Ruthenium

- Allenylidene Complexes as Catalysts for Ring Closing Olefin Metathesis. *Chem. Eur. J.* **2000**, *6*, 1847–1857.
- (38) Castarlenas, R.; Vovard, C.; Fischmeister, C.; Dixneuf, P. H. Allenylidene-to-Indenylidene Rearrangement in Arene-Ruthenium Complexes: A Key Step to Highly Active Catalysts for Olefin Metathesis Reactions. *J. Am. Chem. Soc.* **2006**, *128*, 4079–4089.
- (39) Antonucci, A.; Bassetti, M.; Bruneau, C.; Dixneuf, P. H.; Pasquini, C. Allenylidene to Indenylidene Rearrangement in Cationic p-Cymene Ruthenium(II) Complexes: Solvent, Counteranion, and Substituent Effects in the Key Step toward Catalytic Olefin Metathesis. *Organometallics* **2010**, *29*, 4524–4531.
- (40) Pump, E.; Slugovc, C.; Cavallo, L.; Poater, A. Mechanism of the Ru–Allenylidene to Ru–Indenylidene Rearrangement in Ruthenium Precatalysts for Olefin Metathesis. *Organometallics* **2015**, *34*, 3107–3111.
- (41) Wang, D.; Unold, J.; Bubrin, M.; Frey, W.; Kaim, W.; Buchmeiser, M. R. Ruthenium(IV)—Bis(methallyl) Complexes as UV-Latent Initiators for Ring-Opening Metathesis Polymerization. *ChemCatChem* **2012**, *4*, 1808—1812.
- (42) Webb, D. J.; Hayes, P. G., 1.07 On the Coordination Chemistry of Bis- and Trisphosphinimine Containing Ligands. In *Comprehensive Coordination Chemistry III*; Constable, E. C.; Parkin, G.; Que, L., Jr., Eds. Elsevier: Oxford, 2021; pp 131–157.
- (43) Park, S. V.; Fry, C. G.; Bill, E.; Berry, J. F. A metastable RuIII azido complex with metallo-Staudinger reactivity. *Chem. Commun.* **2020**, *56*, 10738–10741.
- (44) Pawson, D.; Griffith, W. P. Electrophilic behaviour of the nitride ligand in osmium and ruthenium complexes. *Inorg. Nucl. Chem. Lett.* **1974**, *10*, 253–255.
- (45) Phillips, F. L.; Skapski, A. C. X-Ray molecular structure of Ru(NPEt2Ph)Cl3(PEt2Ph)2; a complex with a co-ordinated tertiary phosphineiminato(1–) ion. *J. Chem. Soc., Chem. Commun.* **1974**, *0*, 49–50.
- (46) Pawson, D.; Griffith, W. P. Metal nitrido- and oxo-complexes. Part II. Osmium and ruthenium nitrido-complexes with Group 5 ligands and their reactions. *J. Chem. Soc., Dalton Trans.* **1975**, 417–423.
- (47) Phillips, F. L.; Skapski, A. C. Crystal and molecular structure of trichlorobis (diethylphenylphosphineiminato)ruthenium(IV): a complex with an almost linear Ru–N–P system. *J. Chem. Soc., Dalton Trans.* 1976, 1448–1453.
- (48) Pattacini, R.; Predieri, G.; Tiripicchio, A.; Mealli, C.; Phillips, A. D. Experimental and computational studies on the solvent-controlled cluster isomerism of Ru3(H)(CO)9(NPPh3) and related dynamics. *Chem. Commun.* **2006**, 1527–1529.
- (49) Belletti, D.; Braunstein, P.; Messaoudi, A.; Pattacini, R.; Predieri, G.; Tiripicchio, A. Trapping a pseudo-Hofmann rearrangement on a ruthenium cluster. *Chem. Commun.* **2007**, 141–143.
- (50) Yi; Lam, T. C. H.; Sau, Y.-K.; Zhang, Q.-F.; Williams, I. D.; Leung, W.-H. Electrophilic Ruthenium(VI) Nitrido Complex Containing Kläui's Oxygen Tripodal Ligand. *Inorg. Chem.* **2007**, 46, 7193–7198.
- (51) Ho, C.-M.; Leung, H.-C.; Wu, S.; Low, K.-H.; Lin, Z.; Che, C.-M. Thermal and Photochemical Reactions of Azidoruthenium(III) Complexes of Macrocyclic Tertiary Amines and the Structure of the (Phosphoraniminato)ruthenium(III) Complex trans-[Ru(14-TMC)-(N3)(NPPh3)]+. Eur. J. Inorg. Chem. 2012, 2012, 151–159.
- (52) Ng, H.-Y.; Cheung, W.-M.; Kwan Huang, E.; Wong, K.-L.; Sung, H. H. Y.; Williams, I. D.; Leung, W.-H. Ruthenium chalcogenonitrosyl and bridged nitrido complexes containing chelating sulfur and oxygen ligands. *Dalton Trans.* **2015**, *44*, 18459–18468.
- (53) Bagh, B.; Broere, D. L. J.; Siegler, M. A.; van der Vlugt, J. I. Redox-Active-Ligand-Mediated Formation of an Acyclic Trinuclear Ruthenium Complex with Bridging Nitrido Ligands. *Angew. Chem., Int. Ed.* **2016**, *55*, 8381–8385.
- (54) Wu, X.; Daniliuc, C. G.; Hrib, C. G.; Tamm, M. Phosphoraneiminato tungsten alkylidyne complexes as highly efficient

- alkyne metathesis catalysts. J. Organomet. Chem. 2011, 696, 4147–4151.
- (55) Dehnicke, K.; Krieger, M.; Massa, W. Phosphoraneiminato complexes of transition metals. *Coord. Chem. Rev.* **1999**, *182*, 19–65. (56) Stephan, D. W. The Road to Early-Transition-Metal Phosphinimide Olefin Polymerization Catalysts. *Organometallics*
- 2005, 24, 2548–2560. (57) Stephan, D. W. Sterically Demanding Phosphinimides: Ligands for Unique Main Group and Transition Metal Chemistry. In *Advances in Organometallic Chemistry*; Robert, W.; Anthony, F. H., Eds.; Academic Press, 2006; Vol. 54, pp 267–291.
- (58) LePichon, L.; Stephan, D. W.; Gao, X.; Wang, Q. Iron Phosphinimide and Phosphinimine Complexes: Catalyst Precursors for Ethylene Polymerization. *Organometallics* **2002**, 21, 1362–1366.
- (59) Stephan, D. W.; Stewart, J. C.; Guérin, F.; Courtenay, S.; Kickham, J.; Hollink, E.; Beddie, C.; Hoskin, A.; Graham, T.; Wei, P.; Spence, R. E. v. H.; Xu, W.; Koch, L.; Gao, X.; Harrison, D. G. An Approach to Catalyst Design: Cyclopentadienyl-Titanium Phosphinimide Complexes in Ethylene Polymerization. *Organometallics* **2003**, 22, 1937–1947.
- (60) Guérin, F.; Stewart, J. C.; Beddie, C.; Stephan, D. W. Synthesis, Structure, and Reactivity of the Phosphinimide Complexes (t-Bu3PN)nMX4-n (M = Ti, Zr). Organometallics **2000**, 19, 2994–3000.
- (61) Yue, N.; Hollink, E.; Guérin, F.; Stephan, D. W. Zirconium Phosphinimide Complexes: Synthesis, Structure, and Deactivation Pathways in Ethylene Polymerization Catalysis. *Organometallics* **2001**, 20, 4424–4433.
- (62) Kickham, J. E.; Guérin, F.; Stewart, J. C.; Urbanska, E.; Stephan, D. W. Multiple C-H Bond Activation: Reactions of Titanium-Phosphinimide Complexes with Trimethylaluminum. *Organometallics* **2001**, *20*, 1175–1182.
- (63) Hollink, E.; Wei, P.; Stephan, D. W. The Effects of Activators on Zirconium Phosphinimide Ethylene Polymerization Catalysts. *Organometallics* **2004**, *23*, 1562–1569.
- (64) Hollink, E.; Wei, P.; Stephan, D. W. Group IV phosphinimide amide complexes. Can. J. Chem. 2004, 82, 1634–1639.
- (65) Ghesner, I.; Fenwick, A.; Stephan, D. W. Di-tert-butylbiphenylphosphinimide Titanium and Zirconium Complexes: Pendant Arene–Metal Interactions. *Organometallics* **2006**, *25*, 4985–4995.
- (66) Yadav, K.; McCahill, J. S. J.; Bai, G.; Stephan, D. W. Phosphinimide complexes with pendant hemilabile donors: synthesis, structure and ethylene polymerization activity. *Dalton Trans.* **2009**, 1636–1643.
- (67) Alhomaidan, O.; Beddie, C.; Bai, G.; Stephan, D. W. Titanium complexes of amidophosphinimide ligands. *Dalton Trans.* **2009**, 1991–1998.
- (68) Ramos, A.; Stephan, D. W. Titanium ferrocenyl-phosphinimide complexes. *Dalton Trans.* **2010**, *39*, 1328–1338.
- (69) Reisz, J. A.; Klorig, E. B.; Wright, M. W.; King, S. B. Reductive Phosphine-Mediated Ligation of Nitroxyl (HNO). *Org. Lett.* **2009**, *11*, 2719–2721.
- (70) Jones, C. G.; Asay, M.; Kim, L. J.; Kleinsasser, J. F.; Saha, A.; Fulton, T. J.; Berkley, K. R.; Cascio, D.; Malyutin, A. G.; Conley, M. P.; Stoltz, B. M.; Lavallo, V.; Rodríguez, J. A.; Nelson, H. M. Characterization of Reactive Organometallic Species via MicroED. ACS Cent. Sci. 2019, 5, 1507–1513.
- (71) Aguilar, D.; Bielsa, R.; Soler, T.; Urriolabeitia, E. P. Cycloruthenated Complexes from Iminophosphoranes: Synthesis, Structure, and Reactivity with Internal Alkynes. *Organometallics* **2011**, 30, 642–648.
- (72) Feichtner, K.-S.; Scherpf, T.; Gessner, V. H. Cooperative Bond Activation Reactions with Ruthenium Carbene Complex PhSO2-(Ph2PNSiMe3)C=Ru(p-cymene): Ru=C and N-Si Bond Reactivity. Organometallics 2018, 37, 645–654.
- (73) Sanford, M. S.; Love, J. A.; Grubbs, R. H. Mechanism and Activity of Ruthenium Olefin Metathesis Catalysts. *J. Am. Chem. Soc.* **2001**, *123*, 6543–6554.
- (74) Kiselev, S. A.; Lenev, D. A.; Lyapkov, A. A.; Semakin, S. V.; Bozhenkova, G.; Verpoort, F.; Ashirov, R. V. Reactivity of norbornene

- esters in ring-opening metathesis polymerization initiated by a N-chelating Hoveyda II type catalyst. RSC Adv. 2016, 6, 5177–5183.
- (75) Chu, C. K.; Lin, T.-P.; Shao, H.; Liberman-Martin, A. L.; Liu, P.; Grubbs, R. H. Disentangling Ligand Effects on Metathesis Catalyst Activity: Experimental and Computational Studies of Ruthenium—Aminophosphine Complexes. *J. Am. Chem. Soc.* **2018**, *140*, 5634—5643.
- (76) Grudzień, K.; Trzaskowski, B.; Smoleń, M.; Gajda, R.; Woźniak, K.; Grela, K. Hoveyda—Grubbs catalyst analogues bearing the derivatives of N-phenylpyrrol in the carbene ligand structure, stability, activity and unique ruthenium—phenyl interactions. *Dalton Trans.* **2017**, *46*, 11790—11799.
- (77) Planer, S.; Małecki, P.; Trzaskowski, B.; Kajetanowicz, A.; Grela, K. Sterically Tuned N-Heterocyclic Carbene Ligands for the Efficient Formation of Hindered Products in Ru-Catalyzed Olefin Metathesis. ACS Catal. 2020, 10, 11394–11404.
- (78) Sanford, M. S.; Ulman, M.; Grubbs, R. H. New Insights into the Mechanism of Ruthenium-Catalyzed Olefin Metathesis Reactions. *J. Am. Chem. Soc.* **2001**, *123*, 749–750.
- (79) Michrowska, A.; Bujok, R.; Harutyunyan, S.; Sashuk, V.; Dolgonos, G.; Grela, K. Nitro-Substituted Hoveyda—Grubbs Ruthenium Carbenes: Enhancement of Catalyst Activity through Electronic Activation. *J. Am. Chem. Soc.* **2004**, *126*, 9318—9325.
- (80) Wakamatsu, H.; Blechert, S. A New Highly Efficient Ruthenium Metathesis Catalyst. *Angew. Chem., Int. Ed.* **2002**, *41*, 2403–2405.
- (81) Trzaskowski, B.; Grela, K. Structural and Mechanistic Basis of the Fast Metathesis Initiation by a Six-Coordinated Ruthenium Catalyst. *Organometallics* **2013**, 32, 3625–3630.
- (82) Baer, C. D.; Edwards, J. O.; Kaus, M. J.; Richmond, T. G.; Rieger, P. H. Kinetics of an associative ligand-exchange process: alcohol exchange with arsenate(V) triesters. *J. Am. Chem. Soc.* **1980**, 102, 5793–5798.
- (83) Forcina, V.; García-Domínguez, A.; Lloyd-Jones, G. C. Kinetics of initiation of the third generation Grubbs metathesis catalyst: convergent associative and dissociative pathways. *Faraday Discuss.* **2019**, 220, 179–195.
- (84) Jawiczuk, M.; Janaszkiewicz, A.; Trzaskowski, B. The influence of the cationic carbenes on the initiation kinetics of ruthenium-based metathesis catalysts; a DFT study. *Beilstein J. Org. Chem.* **2018**, *14*, 2872–2880.
- (85) Pump, E.; Cavallo, L.; Slugovc, C. A theoretical view on the thermodynamic cis-trans equilibrium of dihalo ruthenium olefin metathesis (pre-)catalysts. *Monatsh. Chem.* **2015**, *146*, 1131–1141.
- (86) Minenkov, Y.; Occhipinti, G.; Jensen, V. R. Complete Reaction Pathway of Ruthenium-Catalyzed Olefin Metathesis of Ethyl Vinyl Ether: Kinetics and Mechanistic Insight from DFT. *Organometallics* **2013**, 32, 2099–2111.
- (87) Peverati, R.; Truhlar, D. G. M11-L: A Local Density Functional That Provides Improved Accuracy for Electronic Structure Calculations in Chemistry and Physics. *J. Phys. Chem. Lett.* **2012**, 3, 117–124
- (88) Peverati, R.; Truhlar, D. G. Performance of the M11 and M11-L density functionals for calculations of electronic excitation energies by adiabatic time-dependent density functional theory. *Phys. Chem. Chem. Phys.* **2012**, *14*, 11363–11370.
- (89) Arndt, S.; Schrock, R. R.; Müller, P. Synthesis and Reactions of Tungsten Alkylidene Complexes That Contain the 2,6-Dichlorophenylimido Ligand. *Organometallics* **2007**, *26*, 1279–1290.
- (90) Marinescu, S. C.; King, A. J.; Schrock, R. R.; Singh, R.; Müller, P.; Takase, M. K. Simple Molybdenum(IV) Olefin Complexes of the Type Mo(NR)(X)(Y)(olefin). Organometallics 2010, 29, 6816–6828.
- (91) Nascimento, D. L.; Foscato, M.; Occhipinti, G.; Jensen, V. R.; Fogg, D. E. Bimolecular Coupling in Olefin Metathesis: Correlating Structure and Decomposition for Leading and Emerging Ruthenium—Carbene Catalysts. *J. Am. Chem. Soc.* **2021**, *143*, 11072—11079.
- (92) Bailey, G. A.; Foscato, M.; Higman, C. S.; Day, C. S.; Jensen, V. R.; Fogg, D. E. Bimolecular Coupling as a Vector for Decomposition of Fast-Initiating Olefin Metathesis Catalysts. *J. Am. Chem. Soc.* **2018**, *140*, 6931–6944.

- (93) Nascimento, D. L.; Fogg, D. E. Origin of the Breakthrough Productivity of Ruthenium—Cyclic Alkyl Amino Carbene Catalysts in Olefin Metathesis. *J. Am. Chem. Soc.* **2019**, *141*, 19236—19240.
- (94) Musina, E. I.; Balueva, A. S.; Karasik, A. A. Phosphines: Preparation, Reactivity and Applications. In *Organophosphorus Chemistry: Volume 48*; The Royal Society of Chemistry, 2019; Vol. 48, pp 1–63.
- (95) Richel, A.; Delfosse, S.; Cremasco, C.; Delaude, L.; Demonceau, A.; Noels, A. F. Ruthenium catalysts bearing N-heterocyclic carbene ligands in atom transfer radical reactions. *Tetrahedron Lett.* **2003**, *44*, 6011–6015.

| <b>Ⅲ</b> Recommended by ACS | Ш | Recommended | by ACS |
|-----------------------------|---|-------------|--------|
|-----------------------------|---|-------------|--------|

# Catalytic Hydrogenation of Terminal Alkenes by a (PPP) Pincer-Ligated Cobalt(II) Complex

Matthew C. Fitzsimmons, Christine M. Thomas, et al.

MAY 23, 2023 ORGANOMETALLICS

READ 🗹

#### Poly(2,2'-Bibenzimidazole)-Supported Ruthenium Complex: A Recyclable Heterogeneous Catalyst for the Redox Isomerization of Allylic Alcohols to Ketones

Xiaozhong Chen, Feng Li, et al.

DECEMBER 29, 2022

ACS APPLIED POLYMER MATERIALS

READ 🗹

# Unveiling the Latent Reactivity of Cp\* Ligands (C<sub>5</sub>Me<sub>5</sub>-) toward Carbon Nucleophiles on an Iridium Complex

Alejandra Pita-Milleiro, Jesús Campos, et al.

APRIL 03, 2023

INORGANIC CHEMISTRY

READ 🗹

### Retro-Vinylidene Rearrangements of P- and S-Substituted Ruthenium Vinylidene Complexes

Takahiro Iwamoto, Youichi Ishii, et al.

JANUARY 06, 2023

ORGANOMETALLICS

READ 🗹

Get More Suggestions >